Time-Frequency Analysis of Ionospheric Whistler Signals

Miloš Daković, *Member, IEEE*, Milan Ponjavić, *Member, IEEE*, Isidora Stanković, *Student Member, IEEE*, Jonatan Lerga, *Member, IEEE*, Cornel Ioana, *Member, IEEE*,

Abstract — **Time-frequency analysis of the ionospheric whistler signals is presented. Prior to the time-frequency analysis, disturbances caused by power-grid influence and ionospheric tweek and sferic signals are filtered using frequency domain and time domain filtering, respectively. Instantaneous frequency law of whistler signals is then estimated. S-method is used as a time-frequency representation in order to obtain highly concentrated representation without undesired cross-terms. The presented method is applied to the real-life ionospheric signals.**

Keywords — **time-frequency analysis, S-method, ionospheric signals, whistlers**

I. Introduction

LIGHTNINGS are known to radiate intense electromagnetic pulse (EMP) spreading through earth-ionosphere (with ionization being stronger in the upper and weaker in the lower region). This EMP signals are characterized by its frequency content found in the VLF/LF frequency band [1]. It is also known that a portion of the EMP energy propagates upwards in upper atmosphere (in particular, the ionosphere beginning from about 50 km above the Earth's surface) interacting and heating plasma.

Furthermore, some of the energy propagates through the ionosphere into the magnetosphere as a whistler-mode wave. This long duration modulated pulses (with duration up to several seconds), guided by earth magnetosphere and following the geomagnetic field, return to the Earth's surface. Due to its frequency band between 0.3 kHz and 30 kHz, it can be detected by a sensitive audio amplifier with high-frequencies arriving to the amplifier before the lower-pitched signals (known as dispersion effect) [2], [3]. In the time-frequency domain, the whistlers are characterized by a descending arcs. Due to the long path along magnetic field (up to three Earth diameters) dispersive effect are great and they sound like a descending whistle (with a pure tones when they travel along single paths or diffuse if they travel along more complex paths).

Lightnings also produce impulsive short duration signals called sferics (short for "atmospherics") covering wide frequency range from few Hz to millions of Hz. This easy-to-detect signals are heard within the few thousand kilometers from a place of lighting strike due to the ionospheric ducting. Time-frequency representations of the sferics are characterized by vertical lines which correspond to arrival of all of the audio frequencies [4], [5]. They can be described as a sound like cracks, pops, and snaps.

Lightnings also result in tweeks in scenarios when ducted in the earth-ionosphere waveguide with distance significantly higher than several thousand kilometers (and up to half way around the Earth) from a place of lightening discharge. Since ducted over large distance, this VLF radio waves also exhibit dispersion. However, this dispersion is much lower than for the whistlers (few hundred kHz over few thousandths of a second for tweeks when compared to several thousand kHz over second or more for whistlers). Their spectrogram shows vertical lines with a curved sections (called "hooks") at higher frequencies. Tweeks usually last from 10 to 150 ms with "hooks" appearing at about 2 kHz [6]. They can be described as a sound similar to a musical saw being plucked.

Existence of the environmental dispersive channel results in additional complexity of the received signal. The problems caused by the dispersivity are based on the change of the parameters and additional number of modes at the receiving part [7], [8]. Among the other, this inspired us to utilize more advanced time-frequency representations of the ionospheric signal rather than the basic spectrogram. Namely, the S-method was studied for representation of the ionospheric whistler signals in the paper.

The paper is structured as follows. Section II briefly describes time-frequency representations and presents S-method derived from the spectrogram. Real-life signal analysis of ionospheric whistler signal is elaborated on in Section III. Conclusion is found in Section IV.

II. Time-frequency signal representation

Short time Fourier transform (STFT) of a nonstationary discrete signal $x(n)$ is defined as [9]

$$STFT(n,k) = \sum_{m=-N/2}^{N/2-1} w(m)x(n+m)e^{-j2\pi mk/N} \quad (1)$$

where $w(m)$ is analysis window of length N. Spectrogram is the simplest time-frequency representation. It is defined as squared magnitude of the short-time Fourier transform [9], [10]

$$SPEC(n,k) = |STFT(n,k)|^2 \quad (2)$$

Width of the analysis window N plays a crucial role in performance of the STFT and spectrogram. Narrow window will provide good time localization of short components while wide window will provide high frequency resolution for long oscillatory components. Choice of optimal window width is matter of compromise between these two opposite scenarios. This compromise cause smeared time-frequency representation.

In order to improve concentration of the signal components in time-frequency plane quadratic time-frequency distributions are introduced [9]. Signal concentration in time-frequency plane can be measured by norms close to ℓ_1 norm [11]. Although the main goal (good concentration of signal components) is achieved, undesired artifacts, called cross-terms, appear in time-frequency plane. A very simple, and efficient, time-frequency representation, called S-method [9], [10], [12] is introduced in order to avoid cross-terms and remain highly concentrated time-frequency representation. The S-method is defined as

$$SM_L(n,k) = SPEC(n,k)$$
$$+2\sum_{p=1}^{L} \Re\{STFT(n,k-p)STFT^*(n,k+p)\} \quad (3)$$

where L is number of correction terms. For $L = 0$ the S-method is equal to the spectrogram, while for maximal possible $L = N/2 - 1$ pseudo Wigner distribution is obtained.

III. DATA ANALYSIS

Here we will analyze ionospheric signals recorded at the University of Belgrade. Receiver is located within suburban area, so significant low-frequency human-made noise is present. In order to avoid amplifier saturation low frequency noise is filtered out prior to data recording. Filtered signal is sampled with sampling frequency of 44100Hz and recorded in wav file format. The analyzed data file contains 178 seconds of data recorded. Whistler signals are detected (by visual inspection of time-frequency signal content) at $t_0 = 4.5, 30.3, 46.2, 51.0, 75.6, 76.2, 77.8, 104.0, 117.0, 118.0, 119.5, 122.1, 161.0, 165.3$s.

Time frequency representation of whistler signal detected at 4.5s is presented in Fig. 1. It is nonstationary signal covering time range from 4.7s to 5.3s and with frequency decaying from 10kHz down to 3kHz. Time domain representation of the signal is given in the upper subplot and frequency domain representation is on right subplot. Due to significant disturbances the whistler signal cannot be detected from either time or frequency domain representation.

Whistler signals are contaminated by several disturbances. The first one is interference caused by power grid. This kind of interference is almost stationary positioned in frequency at 50Hz and higher order harmonics $k \times 50$Hz, covering frequency range up to 3kHz. The interference is stationary since power grid frequency is controlled and maintained very close to 50Hz.

This disturbance can be removed in frequency domain. Since it is stationary, the disturbance is represented with sharp peaks in frequency domain, but only if we provide good frequency resolution. For this purpose we used large
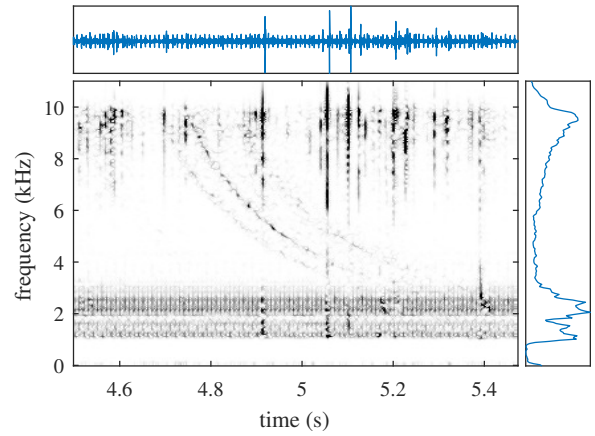

Fig. 1. Event 1. Time-frequency representation of original signal. Signal in the time domain is presented in the subplot above, while signal in the frequency domain is presented right.
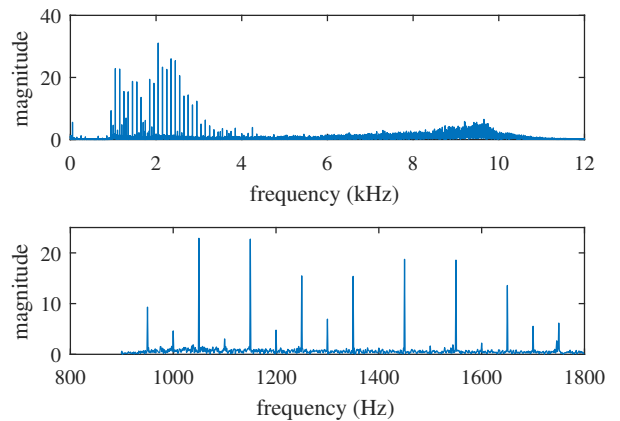

Fig. 2. Frequency domain representation of the received signal. Frequency range from 0kHz to 12kHz is presented in upper subplot. Frequency range from 800Hz to 1800Hz is shown in lower subplot.

part of signal (1s duration) with 44100 samples in total. Fourier transform of signal from Fig. 1 is presented in Fig 2 (upper subplot) with zoomed frequency band up to 3kHz in lower subplot. Now we can easily detect peaks at locations $k \times 50$Hz, remove them and obtain filtered signal using the inverse Fourier transform. Time frequency representation of the filtered signal is presented in Fig. 3. It is obvious that stripe caused by 50Hz harmonics is removed. Note that filtering in time-frequency domain is not suitable for this disturbance since we should use relatively short localization window in order to track nonstationary whistler signal loosing frequency resolution that is required for stationary disturbances filtering. Advanced filtering techniques [13] can further improve results.

Another kind of disturbances are tweeks and sferics. They are direct or surface waves traveling between earth surface and ionosphere. In the time-frequency plane they are represented with almost vertical stripes. This disturbance can be detected (and removed) in time domain, as sharp peaks.

Here we apply very simple time domain filtering. When peak is detected we remove small number of samples around the peak from the signal. Time-frequency representation of the filtered signal is presented in Fig. 4. Now we can see whistler signal components and estimate their
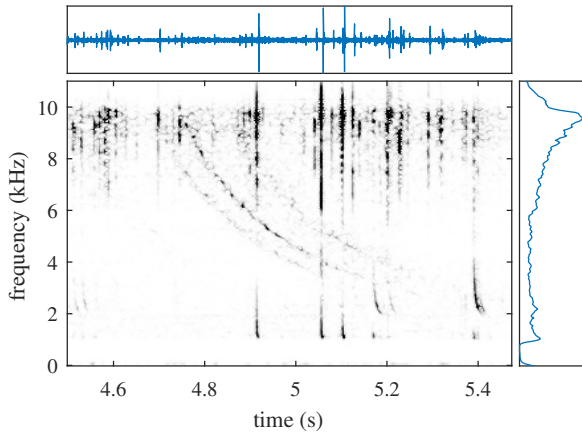
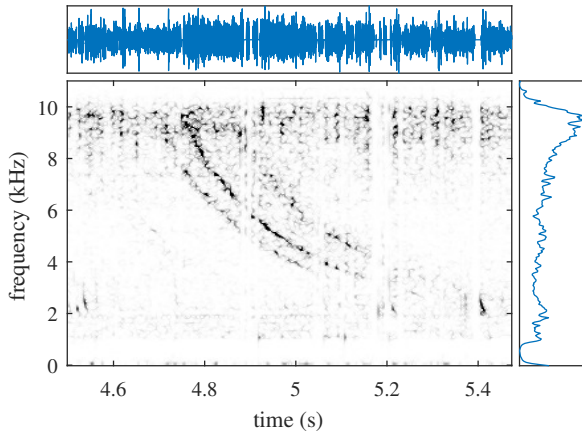Fig. 3. Event 1. Time-frequency representation of filtered signal

Fig. 4. Event 1. Time-frequency representation of signal with pulses removed

parameters.

Now we can examine frequency law of whistler signal. Instantaneous frequency is estimated as position of the local maximum of the obtained time-frequency representation for each time instant [9]. More accurate results can be obtained if we apply advanced instantaneous frequency estimation methods, for example one using the ICI rule applied to a sequence of TFDs calculated for different window widths [15].

Although there are well established mathematical models for whistler signals, most of them does not provide instantaneous frequency law. Here we apply empirical methods and we obtain following relation for whistler signal instantaneous frequency

$$f(t) = \left(\frac{C}{t - t_0}\right)^{3/2} \qquad (4)$$

where t_0 is start time of the discharge event, and $C \approx 173$ is constant.

Ionospheric attenuates frequencies above f_{max} and below f_{min} meaning that observable frequencies, in the range $f_{min} < f(t) < f_{max}$ are within time interval

$$t_0 + \frac{C}{f_{max}^{2/3}} < t < t_0 + \frac{C}{f_{min}^{2/3}}$$

For frequency range from 2kHz to 10kHz expected time range is from 0.37s to 1.09s, with whistler duration of
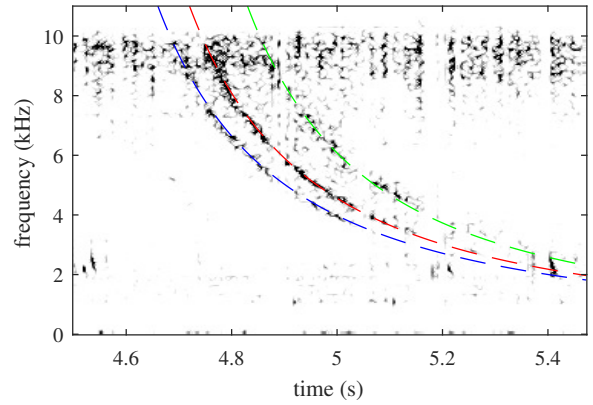

Fig. 5. Event 1. Time-frequency representation of whistler signal along with estimated instantaneous frequency law (dashed lines)

0.72s.

In the considered example we estimated three whistler signals with $t_0^{(1)} = 4.31$s, $t_0^{(2)} = 4.37$s, and $t_0^{(3)} = 4.48$s. Instantaneous frequency laws are plotted with dashed lines over time-frequency signal representation in Fig 5. From this figure we can conclude that estimated instantaneous frequency law highly coincide with real whistler signals.

The analysis is repeated for two more events located at 46.2s and 122.1s. For the first event time-frequency representation of the original signal is presented in Fig. 6 (a), time-frequency representation of filtered signal in Fig. 6 (b), and detected instantaneous frequency laws with $t_0^{(1)} = 45.89$s, $t_0^{(2)} = 45.95$s, and $t_0^{(3)} = 46.07$s, in Fig. 6 (c). Corresponding results for the second event are given in Fig 7 for detected components at $t_0^{(1)} = 121.88$s, $t_0^{(2)} = 121.94$s, and $t_0^{(3)} = 122.07$s.

In all considered cases agreement between signal time-frequency content and estimated instantaneous frequency law is very high.

IV. CONCLUSION

Here we present a simple method for ionospheric whistler waves analysis based on time-frequency analysis of the preprocessed (filtered) signals. The S-method is used as time-frequency representation, while disturbance rejection is implemented in frequency domain, for stationary sinusoidal disturbances, and in time-domain for short pulse disturbances. Instantaneous frequency law of the whistler signal is then estimated. The presented method can be used for whistler detection and estimation of whistler signal parameters. The method is applied to the real-life signals. It is shown that empirically proposed instantaneous frequency law highly correspond to the measured data.

REFERENCES

[1] J. Lichtenberger, C. Ferencz, L. Bodnár, D. Hamar, and P. Steinbach. "Automatic whistler detector and analyzer system: Automatic whistler detector," *Journal of Geophysical Research: Space Physics*, vol. 113, no. A12 (2008).

[2] M. Hayakawa, "Whistlers," *In Handbook of Atmospheric Electrodynamics* (1995), pp. 155-193. CRC Press, 2017.

[3] N. V. Cherneva, V. P. Sivokon, and I. V. Agranat, "Spectral characteristics of whistlers." *In Problems of Geocosmos: Proc. of the 9th Int. Conf.*, St. Petersburg, pp. 212-217, 2012.

[4] D. Mihovilović, and R. N. Bracewell. "Whistler analysis in the time-frequency plane using chirplets." *Journal of Geophysical Research: Space Physics* vol. 97, no. A11 (1992), pp. 17199-17204.
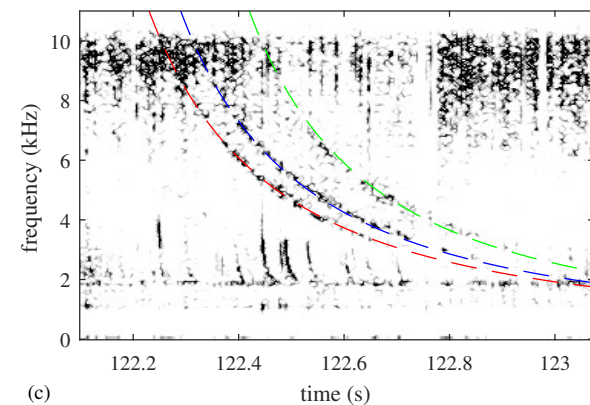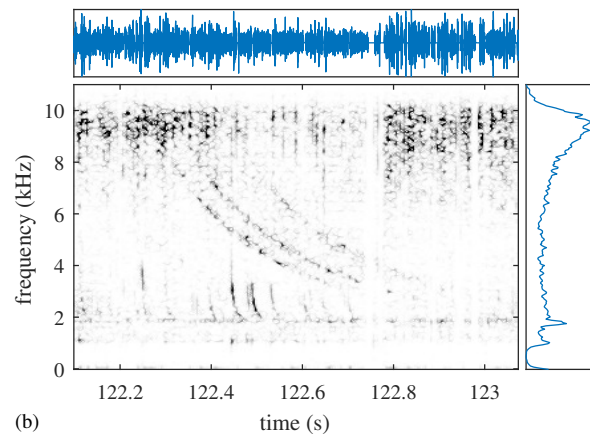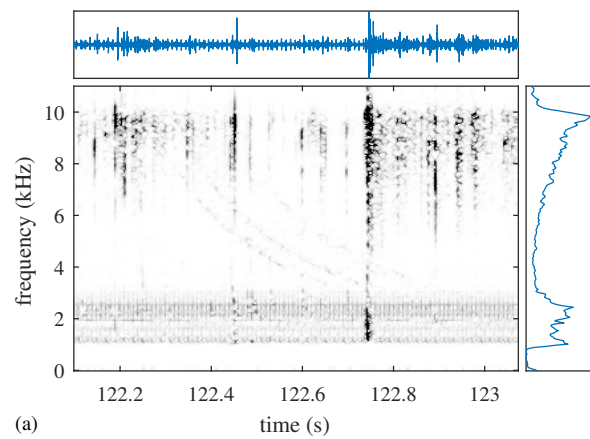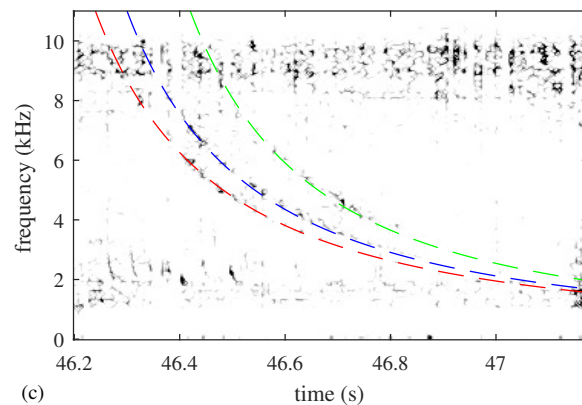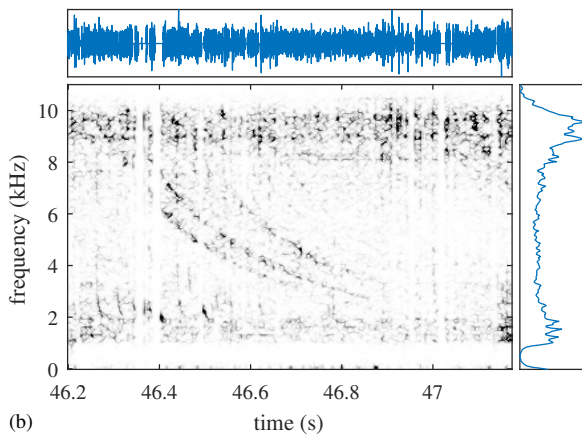
Fig. 6. Event 2: (a) Time-frequency representation of original signal; (b) Time-frequency representation of filtered signal; (c) Time-frequency representation of whistler signal along with estimated instantaneous frequency law (dashed lines)
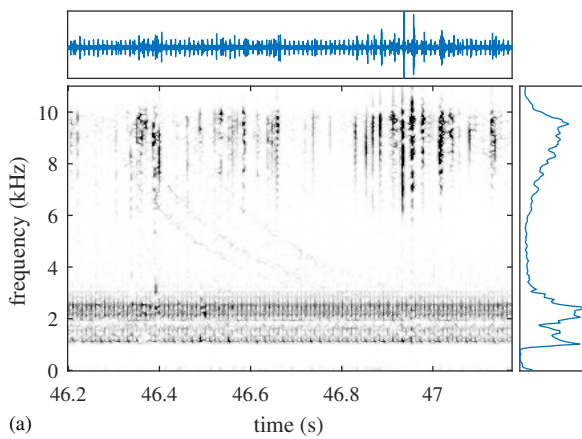

Fig. 7. Event 3: (a) Time-frequency representation of original signal; (b) Time-frequency representation of filtered signal; (c) Time-frequency representation of whistler signal along with estimated instantaneous frequency law (dashed lines)

[5] S. Close, A. Fletcher, M. Dunham, and I. Linscott. "Coherent matched filter signal-processing algorithms for probing the ionosphere using broadband RF data." *Journal of Geophysical Research: Space Physics*, vol. 116, no. A12 (2011).

[6] M. Parrot, and J. Chum. "Propagation spectrograms of whistler-mode radiation from lightning," *IEEE Transactions on Plasma Science*, vol. 36, no. 4 (2008), pp. 1166-1167.

[7] I. Stanković, M. Daković, and C. Ioana, "Decomposition of Signals in Dispersive Channels using Dual Polynomial Fourier Transform," *6th Mediterranean Conference on Embedded Computing MECO*, Bar, Montenegro, June 2017

[8] I. Stanković, C. Ioana, and M. Daković, "Model-based decomposition of acoustic signals in dispersive environment," *26th Symposium GRETSI 2017*, September 5-8, Juan-les-Pins, France

[9] L. Stanković, M. Daković and T. Thayaparan, *Time–Frequency Signal Analysis with Application*, Artech House, 2013

[10] LJ. Stanković, S. Stanković, and M. Daković, "From the STFT to the Wigner distribution," *IEEE Signal Processing Magazine*, vol.

31, no. 3, May 2014, pp. 163-174

[11] LJ. Stanković, "A measure of some time-frequency distributions concentration," *Signal Processing*, vol. 81, no. 3, Mar. 2001, pp. 621-631.

[12] LJ. Stanković, "A method for time-frequency signal analysis," *IEEE Transactions on Signal Processing*, vol. 42, no. 1, Jan.1994, pp. 225-229.

[13] M. Bošković, T. B. Šekara, M. R. Rapaić, B. Lutovac, M. Daković and V. Govedarica, "Novel band-pass and notch filter with dynamic damping of fractional order," *25th Telecommunication Forum (TELFOR)*, Belgrade, 2017, pp. 1-4.

[14] B. Gašpar, D. Jurišić and B. Lutovac, "Narrow BP active filters with reduced noise and sensitivity using current conveyors," *2nd Mediterranean Conference on Embedded Computing (MECO)*, Budva, 2013, pp. 200-203.

[15] J. Lerga, and V. Sučić. "Nonlinear IF estimation based on the pseudo WVD adapted using the improved sliding pairwise ICI rule," *IEEE Signal Processing Letters*, vol. 16, no. 11 (2009), pp. 953-956.